IL NUOVO CIMENTO **45 C** (2022) 76
DOI 10.1393/ncc/i2022-22076-9

COMMUNICATIONS: SIF Congress 2021

Interplay of multiple degrees of freedom in strained VO_2 films

A. D'ELIA([1])([2])

([1]) *ISM-CNR, Sezione di Trieste - Trieste, Italy*
([2]) *RICMASS, Rome International Center for Material Science - Roma, Italy*

received 31 January 2022

Summary. — VO_2 is a strongly correlated electron system that undergoes a reversible Metal-Insulator transition (MIT) triggered by temperature. The MIT is also coupled with a structural phase transition, from monoclinic insulator to tetragonal metal, therefore, the physical nature of the MIT itself has been long debated to be a Mott-Hubbard and a Peierls transition. In this contribution, VO_2 thin films deposited on $TiO_2(001)$ have been studied by synchrotron radiation spectrosocopies in order to investigate the strain effect on the MIT properties. The interplay of the lattice, orbital and electron correlation degrees of freedom and their influence on the MIT will be highlighted.

1. – Introduction

Transition metal oxides (TMO) are an extremely appealing class of materials, since they exhibit a wide range of technologically appealing properties. For example, the high temperature superconductivity shown by cuprates [1], the high work function of MoO_3 [2] and the metal insulator transition (MIT) of VO_2 [3] are just some examples of relevant properties in modern technology. All these unique features of TMO are given by the interplay between the *nd* electrons and the large variety of oxidation state and lattice configurations allowed in these materials [4]. In this work the focus will be on VO_2 and how the MIT is influenced by the strain, orbital and electron correlation degrees of freedom. VO_2 is a strongly correlated electron system and it is a prototypical phase change material. It undergoes a reversible MIT triggered by temperature at 67 °C in bulk crystal. The MIT is accompanied by a structural phase transition (SPT), switching from a low temperature monoclinic insulator to a high temperature tetragonal metal [5,6]. The concurrent phenomenological expression of MIT and SPT has created a hot debate in literature for decades since VO_2 behaviour could be modelled as both a Mott-Hubbard or a Peierls insulator [6,7]. However, in the last ten years a lot of progresses have been made in the field of sample synthesis [8,9], investigation techniques [10-12] and theoretical approaches [13]. The spreading of epitaxial growth of thin films allowed elucidating the

role of orbital population and strain in the lattice on the MIT [14]. On the other hand, the improved precision and reliability of time resolved techniques allowed unveiling the predominant role of the electron-electron correlation on the transition [15, 16]. Nevertheless, the interplay between orbital population, lattice strain and electron correlation are not completely understood. In this contribution, this intricate problem has been studied with the use of advanced spectroscopic techniques like resonant photoemission and X-ray absorption in order to probe multiple degrees of freedom at the same time. The investigated samples are a set of VO_2 thin films of 8, 16, 32 nm, deposited on a $TiO_2(001)$ substrate. The results obtained show an intimate connection between sample thickness, orbital hierarchy, metallicity and electron correlation in VO_2.

2. – Experimental

All the data showed in this contribution have been acquired on the ALOISA beamline [17] at the Elettra synchrotron radiation facility. More details on the experimental condition can be found in [18]. The VO_2 samples have been produced using molecular beam epitaxy [8] in collaboration with the University of Science and Technology of China, Hefei.

3. – Discussion

The peculiar properties of VO_2 MIT can be understood in terms of its band structure. In the metallic phase each vanadium site is surrounded by slightly distorted oxygen octahedral. The crystal field splits the degenerate 3d manifold into three t_{2g} and two e_g^σ levels. The orthorhombic ligands distortion further splits the t_{2g} levels in one singly degenerate a_{1g} and two e_g^π levels. In the Goodenough model [6] V 3d and O 2p orbitals hybridization generates bonds of σ and π symmetry. The respective unoccupied levels are identified in literature as π^*(e_g^π character) and σ^* (e_g^σ character). The a_{1g} orbital is populated by unpaired 3d electrons and is often referred to as $d_{||}$ [6]. In the metallic phase both $d_{||}$ and π^* populate Fermi level. The relative $d_{||}$ /π^* population of FL is dictated by the energy hierarchy of these two orbitals. In bulk VO_2, the $d_{||}$ is more populated with respect to π^*. $d_{||}$ is strongly anisotropic and oriented along the metallic phase c axis, while π^* is more isotropic.

The effect of strain over the band structure of VO_2 is very complex and depends on the crystal orientation on which it is applied. In this work only the strain along the tetragonal (001) direction is considered. The interested reader can find additional information in [19].

Epitaxial growth of thin films allows to impress tensile or compressive strain on VO_2. TiO_2 rutile has the same crystal structure of the metallic phase of VO_2, but with larger lattice parameters. As a consequence, the thin VO_2 films grown on $TiO_2(001)$ substrate will suffer tensile strain in the ab plane as well as compressive strain along the c direction [19]. The lattice mismatch between VO_2 and TiO_2 is of 0.86% in the ab plane [20].

The change of the interatomic distances influences the electronic structure as shown in fig. 1. In the metallic phase, the reduction of the c axis increases the V3d-V3d wave function overlapping by up-shifting in energy the $d_{||}^*$ band. At the same time, the distance between apical oxygen and central vanadium atom increases, resulting in a destabilization of the π^* that is downshifted in energy. The overall result is a change in the orbital hierarchy and thus of the relative band filling at FL. With respect to the

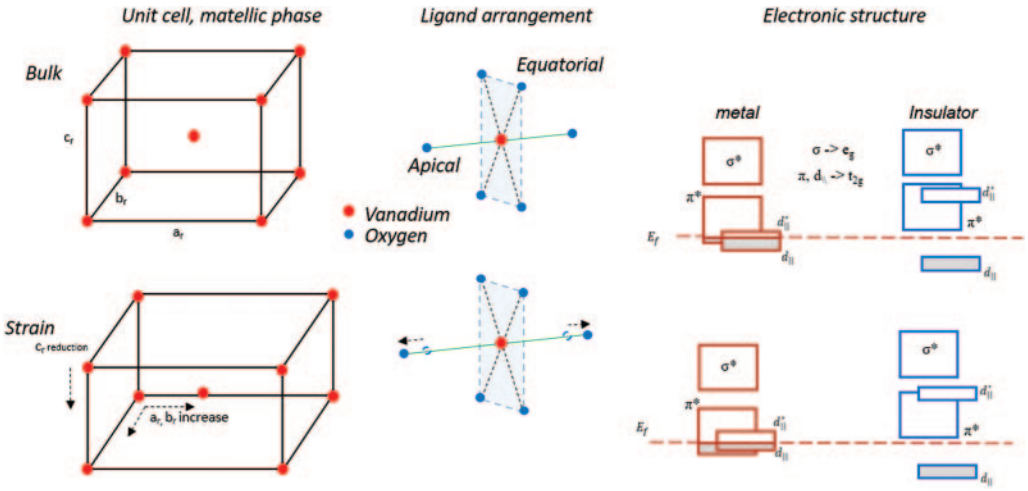

Fig. 1. – Block diagram of the evolution of the unit cell atomic distances, ligands arrangement and electronic structure form bulk VO_2 to a strained film. Only the unit cell of the metallic phase is reported for the sake of simplicity. The effect of strain on the unit cell is extreme for the sake of visualization.

bulk VO_2, a strained film in the metallic phase will have the π^* more populated, and viceversa for the $d^*_{||}$ band [14].

Since π^* and $d^*_{||}$ have mostly V 3d character, the changes of the electronic structure across the MIT can be tracked using X-ray absorption spectroscopy and resonant photoemission at the V L edges and O K edge [21-24].

4. – Results

4˙1. *XANES*. – In order to probe the strain effect on the orbital hierarchy inversion across the MIT, XANES spectra of the VO_2 film have been recorded using Auger yield. The Auger chosen is the O KVV (kinetic energy 507 eV) in order to minimize the V L edges contribution to the oxygen K edge line shape [23]. The recorded spectra in both metallic and insulating phases across the MIT are displayed in fig. 2 along with the difference spectra.

The major changes across the MIT are observed in the energy region corresponding to the π^* and $d^*_{||}$ orbitals as confirmed by a previous XANES investigation at the O K edge [25]. The difference spectra are calculated as the intensity difference between the XANES spectra of the insulating phase minus the XANES spectra of the metallic phase. The spectra in both phases are normalized to σ^* before subtraction, since σ^* is not involved in the spectral weight transfer across the MIT. The difference spectra show an evolution as a function of the film thickness.

The negative contribution around 529.5 eV is decreasing while decreasing the thickness, on the other hand, the positive contribution around 530.6 eV increases. This suggests that the orbital hierarchy inversion is gradually increasing concurrently with film thickness decrease, *i.e.*, strain increases. The reduction of the negative contribution in the difference spectra can be associated with the bandwidth shrinking in the metallic phase of VO_2 under the effect of tensile strain in the ab plane [14]. In the same way, the

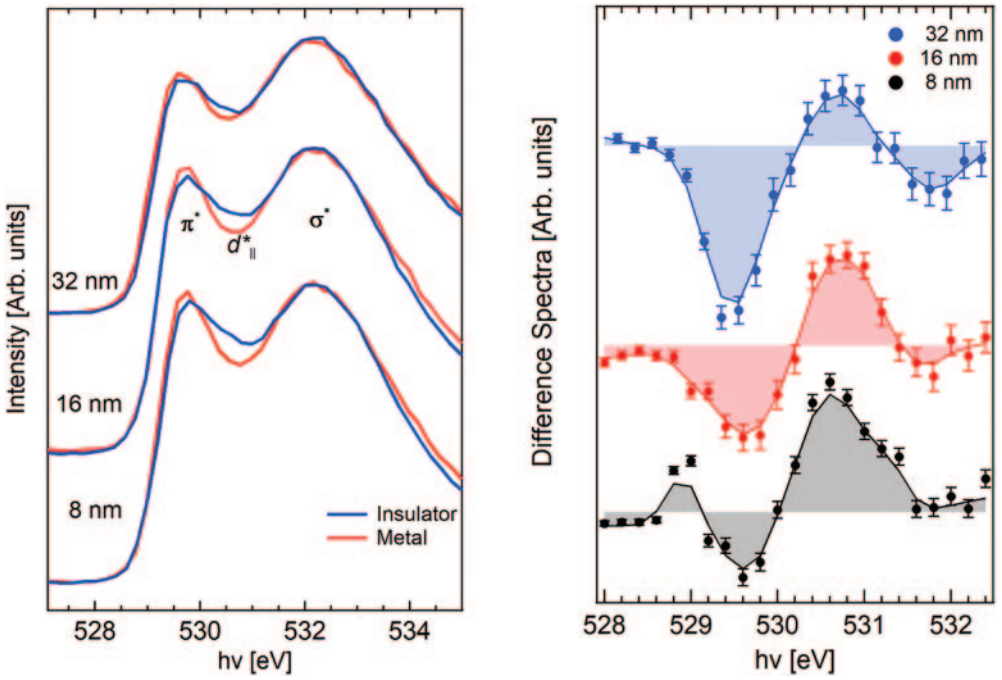

Fig. 2. – Left panel: O K edge XANES spectra of the 32, 16, 8 nm thin films acquired in the metallic (red) and insulating phase (blue). Right panel: difference spectra calculated as the intensity difference between the O K edge spectra of the insulating and metallic phase. Figure adapted with permission from [18].

increasing of the positive contribution and the appearance of a shoulder around 531 eV in the 8 nm film point out the increased $d_{||}$-$d^*_{||}$ energy separation in the insulating phases of strained VO_2. These difference spectra are therefore a clear indication of the thickness effect on the band structure of VO_2 across the phase transition, confirming the hierarchy inversion in the metallic phase and the increased $d_{||}$-$d^*_{||}$ energy separation in the insulating phase [18].

4˙2. *Resonant photoemission.* – These results from XANES measurements are crucial, since they prove the orbital hierarchy inversion without the need of polarization dependent measurements. Nevertheless, XANES can only provide information about the unoccupied density of states. In order to study how the density of state evolves across the phase transition and as a function of strain, it is necessary to use photo-emission spectroscopy. Resonant photoemission (ResPES) spectroscopy has been performed on all the three VO_2 samples, tuning the photon energy across the V L_2 and L_3 edges.

The advantage of using ResPES relies in the enhanced chemical sensitivity with respect to off-resonance photoemission. By tuning the photon energy across a resonance of the system it is possible to coherently enhance the signal from a specific chemical species. Since the electrons involved in the MIT in VO_2 are mainly V 3d electrons around FL [26], ResPES across the V L edges, provides an ideal tool to study the band dynamics across the transition.

The ResPES maps of the VO_2 thin films in the binding energy region [3,−0.5] eV and with photon energy across the V L edges (hv = 512–529 eV) are reported in fig. 3.

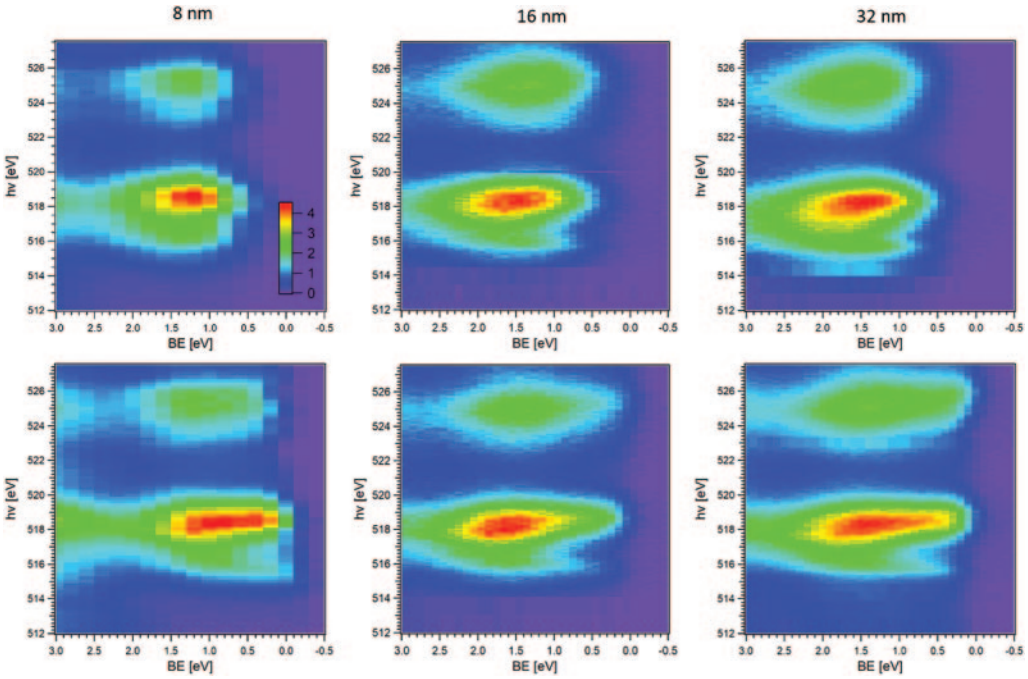

Fig. 3. – ResPES maps for the VO_2 films across the V L_3 edge. Top row, insulating phase, bottom row, metallic phase. Figure reproduced with permission from [26].

The intensity maps clearly show the resonant enhancement of the photo-emission spectra when the photon energy is tuned through a resonance. The differences between metallic and insulating phases are most evident at FL (binding energy = 0 eV), which is populated when VO_2 is a metal, while it is empty when it is an insulator.

ResPES is also very useful to probe the metallicity of thin films, *i.e.*, ability to efficiently screen an electric field [27-29]. The intensity of the ResPES spectra when the photon energy is tuned on the maximum of the resonance can be linked to the screening parameter (inverse of the Debye screening length) using the following equation:

$$\frac{I}{I_0} \propto \frac{1}{\lambda_D} = L_s, \tag{1}$$

where I is the intensity of the ResPES spectra at the maximum of the resonance, I_0 is the incident photon flux, λ_D is the Debye screening length and L_s is the screening parameter.

The spectra acquired at the maximum of the V L_3 resonance for the 8,16 and 32 nm thin films, in both insulating and metallic phase, are reported in fig. 4.

It is clearly observable a trend in the intensity ratio between the insulating and metallic phase as a function of the film thickness. By using the previous equation it is therefore possible to calculate the ratio between the screening parameter of the insulating and metallic phase as a function of film thickness. This quantity, reported in the right panel of fig. 4, tells us how the metallicity of the film changes reducing the film thickness. It is evident that when reducing the film thickness, *i.e.*, increasing the strain,

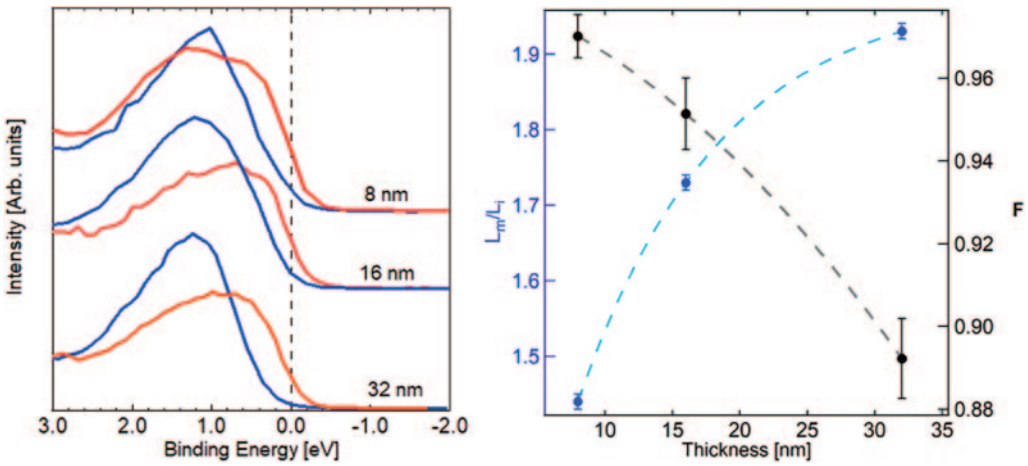

Fig. 4. – Left panel: Resonant photoemission spectra of the $VO_2$2 films in the metallic (red) and insulating (blue) phase acquired at the maximum of the V L_3 edge (photon energy 518.4 eV). Right panel: evolution of VO_2 metallicity (L_m/L_i) and filling factor F as a function of VO_2 film thickness. Figure adapted with permission from [18].

the metallicity of the film decreases. This is also confirmed by observing the filling ratio F, calculated by the XANES spectra and defined as $\frac{\pi*+d_{||}}{\sigma*}$ [18].

The F ratio gives us information about the overall number of empty states available in the π^* and $d^*_{||}$ bands [18]. In the right panel of fig. 4 it is observable how the number of empty states in the π^* and $d^*_{||}$ bands increases as the film thickness decreases. This is coherent with the trend of the metallicity as a function of the film thickness, in fact an increased number of empty states corresponds to a reduced FL population and therefore to a reduction of the metallicity. This points out a mechanism of depopulation of FL as the film thickness is reduced, *i.e.*, as the strain increases the number of electrons populating FL is reduced and this influences the electron-electron correlation.

Photoemission makes it possible to probe the effective electron correlation in a strongly correlated material as shown in [30] fitting the two components of the VB close to FL in the metallic phase. As shown in fig. 5, the VB of the metallic phase of VO_2 shows two components called L (ligand-hole) and C (coherent-hole) generated by two different final state screening channels [31].

L is a local screening channel where the photo-hole on the V3d shell is screened by the electrons belonging to surrounding oxygen atoms. On the other hand, C is a delocalized mechanism of the free electrons that cooperatively screen the V 3d hole created by the photoemission process. Within the Birkman-Rice picture [30,32] it is possible to calculate the ratio between the effective electron correlation and the critical electron correlation from the intensity of the C and L contributions as follows:

$$\frac{\int I_C(E)\,\mathrm{d}E}{\int I_C(E)\,\mathrm{d}E + \int I_L(E)\,\mathrm{d}E} = 1 - \left(\frac{U_{eff}}{U_C}\right)^2, \tag{2}$$

where $I_C(E)$ is the intensity of the C fitting component, $I_L(E)$ is the intensity of the L component, U_{eff} is the effective electron correlation in the sample and U_C is the critical electron correlation for which the MIT takes place.

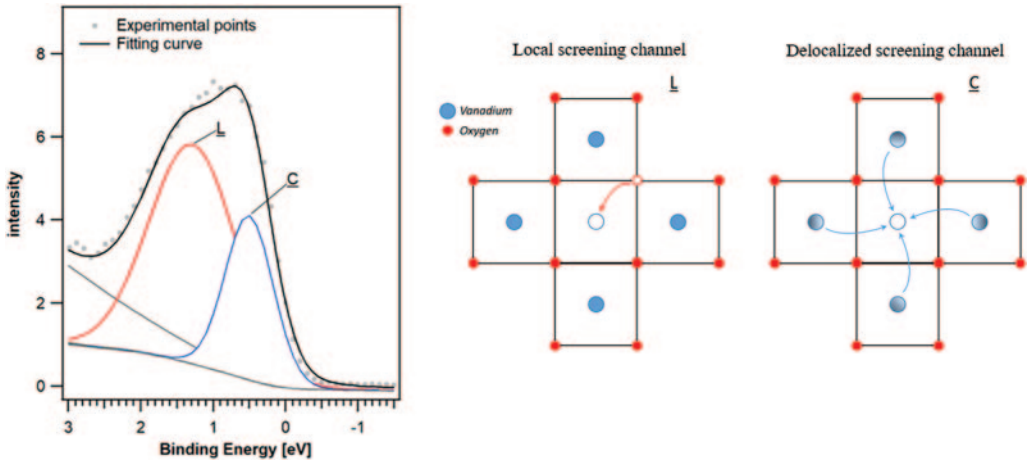

Fig. 5. – Left panel: example of VB fit for the 32 nm film. The experimental points of the VB of the 32 nm film in the metallic phase (hv = 518.4 eV) are reported in grey, the fitting curves are reported in black, and the fitting components are reported in red and blue. The right panel shows the schematic representation of the ligand-hole and coherent-hole screening channel.

Using this equation it is therefore possible to calculate the effective electron correlation present in the medium. Applying this procedure to the whole set of film it has been possible to trace a phase diagram of the critical temperature *vs.* $\frac{U_{eff}}{U_C}$ as depicted in fig. 6.

The data point out that the electron correlation decreases along with the critical temperature. This is expected considering that T_c is related to the energy necessary to

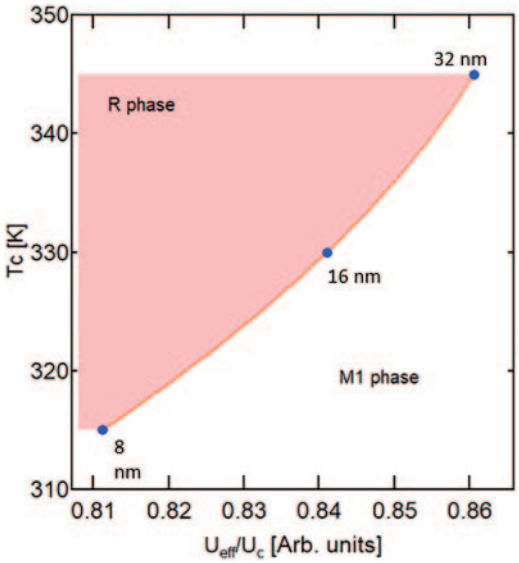

Fig. 6. – Phase diagram T_c *vs.* $\frac{U_{eff}}{U_C}$.

overcome the electron correlation and therefore allowing the flow of electrical current in the material and thus triggering the MIT. These results establish a direct correlation between Fermi level population strain and e-e correlation, where strain emerges as the degree of freedom that regulates all these properties.

5. – Conclusion

This work demonstrates the crucial role of strain in the control of VO_2 MIT features. Using XANES spectroscopy performed at the O K edge, it has been possible to track the orbital hierarchy inversion in the VO_2 metallic phase as a function of film thickness, *i.e.*, applied strain. ResPES investigation at the V L edges revealed that the change in the relative population of π^* and $d^*_{||}$ at FL is accompanied by a reduction of the number of free electron populating FL, and therefore of the metallicity of the film. This unveils a crucial mechanism: strain allows to tune the population of FL and therefore the electron-electron correlation and in last stance the critical temperature of the transition. The evidences collected allow us to identify strain as the key parameter that controls and regulates the balance between multiple degrees of freedom, like orbital hierarchy, metallicity and electron correlation. This study reveals the pivotal role of strain in regulating the properties of the MIT in VO_2 highlighting the importance of taking into account the contribution of multiple degrees of freedom in order to control the properties of strongly correlated materials.

* * *

The author acknowledges the contribution of Dr. Cesare Grazioli, Prof. Albano Cossaro, Dr. Bowen Li, Prof. Chongwen Zou, Dr. Javad Rezvani, Dr. Augusto Marcelli, and Dr. Marcello Coreno. Without their valuable help in the different stages of this project it would have been impossible to obtain these results. Again, thank you.

REFERENCES

[1] Makarov I., Gavrichkov V., Shneyder E., Nekrasov I., Slobodchikov A., Ovchinnikov S. and Bianconi A., *J. Supercond. Novel Magn.*, **32** (2019) 1927.
[2] Macis S., Aramo C., Bonavolontà C., Cibin G., D'Elia A., Davoli I., De Lucia M., Lucci M., Lupi S., Miliucci M. *et al.*, *J. Vacuum Sci. Technol. A*, **37** (2019) 021513.
[3] Brahlek M., Zhang L., Lapano J., Zhang H.-T., Engel-Herbert R., Shukla N., Datta S., Paik H. and Schlom D. G., *MRS Commun.*, **7** (2017) 27.
[4] Zhou Y. and Ramanathan S., *Proc. IEEE*, **103** (2015) 1289.
[5] Morin F., *Phys. Rev. Lett.*, **3** (1959) 34.
[6] Goodenough J. B., *J. Solid State Chem.*, **3** (1971) 490.
[7] Zylbersztejn A. and Mott N. F., *Phys. Rev. B*, **11** (1975) 4383.
[8] Fan L., Chen S., Luo Z., Liu Q., Wu Y., Song L., Ji D., Wang P., Chu W., Gao C. *et al.*, *Nano Lett.*, **14** (2014) 4036.
[9] Lee D., Chung B., Shi Y., Kim G.-Y., Campbell N., Xue F., Song K., Choi S.-Y., Podkaminer J., Kim T. *et al.*, *Science*, **362** (2018) 1037.
[10] Paez G. J., Singh C. N., Wahila M. J., Tirpak K. E., Quackenbush N. F., Sallis S., Paik H., Liang Y., Schlom D. G., Lee T.-L. *et al.*, *Phys. Rev. Lett.*, **124** (2020) 196402.
[11] Evlyukhin E., Howard S. A., Paik H., Paez G. J., Gosztola D. J., Singh C. N., Schlom D. G., Lee W.-C. and Piper L. F., *Nanoscale*, **12** (2020) 18857.
[12] Morrison V. R., Chatelain R. P., Tiwari K. L., Hendaoui A., Bruhács A., Chaker M. and Siwick B. J., *Science*, **346** (2014) 445.

[13] Grandi F., Amaricci A. and Fabrizio M., *Phys. Rev. Res.*, **2** (2020) 013298.
[14] Aetukuri N. B., Gray A. X., Drouard M., Cossale M., Gao L., Reid A. H., Kukreja R., Ohldag H., Jenkins C. A., Arenholz E. *et al.*, *Nat. Phys.*, **9** (2013) 661.
[15] Wall S., Yang S., Vidas L., Chollet M., Glownia J. M., Kozina M., Katayama T., Henighan T., Jiang M., Miller T. A. *et al.*, *Science*, **362** (2018) 572.
[16] Jager M. F., Ott C., Kraus P. M., Kaplan C. J., Pouse W., Marvel R. E., Haglund R. F., Neumark D. M. and Leone S. R., *Proc. Natl. Acad. Sci. U.S.A.*, **114** (2017) 9558.
[17] Costantini R., Stredansky M., Cvetko D., Kladnik G., Verdini A., Sigalotti P., Cilento F., Salvador F., De Luisa A., Benedetti D. *et al.*, *J. Electron Spectrosc. Relat. Phenom.*, **229** (2018) 7.
[18] D'Elia A., Grazioli C., Cossaro A., Li B., Zou C., Rezvani S., Pinto N., Marcelli A. and Coreno M., *Appl. Surface Sci.*, **540** (2021) 148341.
[19] Fan L., Chen S., Liao G., Chen Y., Ren H. and Zou C., *J. Phys.: Condens. Matter*, **28** (2016) 255002.
[20] Kittiwatanakul S., Wolf S. A. and Lu J., *Appl. Phys. Lett.*, **105** (2014) 073112.
[21] Abbate M., De Groot F., Fuggle J., Ma Y., Chen C., Sette F., Fujimori A., Ueda Y. and Kosuge K., *Phys. Rev. B*, **43** (1991) 7263.
[22] Eguchi R., Taguchi M., Matsunami M., Horiba K., Yamamoto K., Ishida Y., Chainani A., Takata Y., Yabashi M., Miwa D. *et al.*, *Phys. Rev. B*, **78** (2008) 075115.
[23] Marcelli A., Coreno M., Stredansky M., Xu W., Zou C., Fan L., Chu W., Wei S., Cossaro A., Ricci A. *et al.*, *Condens. Matter*, **2** (2017) 38.
[24] D'Elia A., Rezvani S., Cossaro A., Stredansky M., Grazioli C., Li B., Zou C., Coreno M. and Marcelli A., *J. Supercond. Novel Magn.*, **33** (2020) 2383.
[25] Quackenbush N., Paik H., Wahila M., Sallis S., Holtz M., Huang X., Ganose A., Morgan B., Scanlon D. O., Gu Y. *et al.*, *Phys. Rev. B*, **94** (2016) 085105.
[26] D'Elia A., Grazioli C., Cossaro A., Li B., Zou C., Rezvani S. J., Marcelli A. and Coreno M., *Condens. Matter*, **5** (2020) 72.
[27] Dowben P. A., *Surface Sci. Rep.*, **40** (2000) 151.
[28] McIlroy D., Waldfried C., Zhang J., Choi J.-W., Foong F., Liou S. and Dowben P. A., *Phys. Rev. B*, **54** (1996) 17438.
[29] Li D., Zhang J., Lee S. and Dowben P. A., *Phys. Rev. B*, **45** (1992) 11876.
[30] Takami H., Kanki T., Ueda S., Kobayashi K. and Tanaka H., *Phys. Rev. B*, **85** (2012) 205111.
[31] Mossanek R. and Abbate M., *Phys. Rev. B*, **74** (2006) 125112.
[32] Brinkman W. F. and Rice T. M., *Phys. Rev. B*, **2** (1970) 4302.